Elsevier instructions for the preparation of a 2-column format camera-ready paper in LaTeX

P. de Groot[a*], R. de Maas[a†], X.-Y. Wang[b] and A. Sheffield[a‡]

[a]Mathematics and Computer Science Section, Elsevier Science B.V.,
P.O. Box 103, 1000 AC Amsterdam, The Netherlands

[b]Economics Department, University of Winchester,
2 Finch Road, Winchester, Hampshire P3L T19, United Kingdom

These pages provide you with an example of the layout and style for 100% reproduction which we wish you to adopt during the preparation of your paper. This is the output from the LaTeX document class you requested.

1. FORMAT

Text should be produced within the dimensions shown on these pages: each column 7.5 cm wide with 1 cm middle margin, total width of 16 cm and a maximum length of 19.5 cm on first pages and 21 cm on second and following pages. The LaTeX document class uses the maximum stipulated length apart from the following two exceptions (i) LaTeX does not begin a new section directly at the bottom of a page, but transfers the heading to the top of the next page; (ii) LaTeX never (well, hardly ever) exceeds the length of the text area in order to complete a section of text or a paragraph. Here are some references: [1,2].

1.1. Spacing

We normally recommend the use of 1.0 (single) line spacing. However, when typing complicated mathematical text LaTeX automatically increases the space between text lines in order to prevent sub- and superscript fonts overlapping one another and making your printed matter illegible.

1.2. Fonts

These instructions have been produced using a 10 point Computer Modern Roman. Other recommended fonts are 10 point Times Roman, New Century Schoolbook, Bookman Light and Palatino.

2. PRINTOUT

The most suitable printer is a laser or an inkjet printer. A dot matrix printer should only be used if it possesses an 18 or 24 pin printhead ("letter-quality").

The printout submitted should be an original; a photocopy is not acceptable. Please make use of good quality plain white A4 (or US Letter) paper size. *The dimensions shown here should be strictly adhered to: do not make changes to these dimensions, which are determined by the document class.* The document class leaves at least 3 cm at the top of the page before the head, which contains the page number.

Printers sometimes produce text which contains light and dark streaks, or has considerable lighting variation either between left-hand and right-hand margins or between text heads and bottoms. To achieve optimal reproduction quality, the contrast of text lettering must be uniform,

*Footnotes should appear on the first page only to indicate your present address (if different from your normal address), research grant, sponsoring agency, etc. These are obtained with the `\thanks` command.

†For following authors with the same address use the `\addressmark` command.

‡To reuse an addressmark later on, label the address with an optional argument to the `\address` command, e.g. `\address[MCSD]`, and repeat the label as the optional argument to the `\addressmark` command, e.g. `\addressmark[MCSD]`.

sharp and dark over the whole page and throughout the article.

If corrections are made to the text, print completely new replacement pages. The contrast on these pages should be consistent with the rest of the paper as should text dimensions and font sizes.

3. TABLES AND ILLUSTRATIONS

Tables should be made with LaTeX; illustrations should be originals or sharp prints. They should be arranged throughout the text and preferably be included *on the same page as they are first discussed*. They should have a self-contained caption and be positioned in flush-left alignment with the text margin within the column. If they do not fit into one column they may be placed across both columns (using `\begin{table*}` or `\begin{figure*}` so that they appear at the top of a page).

3.1. Tables

Tables should be presented in the form shown in Table 1. Their layout should be consistent throughout.

Horizontal lines should be placed above and below table headings, above the subheadings and at the end of the table above any notes. Vertical lines should be avoided.

If a table is too long to fit onto one page, the table number and headings should be repeated above the continuation of the table. For this you have to reset the table counter with `\addtocounter{table}{-1}`. Alternatively, the table can be turned by 90° ('landscape mode') and spread over two consecutive pages (first an even-numbered, then an odd-numbered one) created by means of `\begin{table}[h]` without a caption. To do this, you prepare the table as a separate LaTeX document and attach the tables to the empty pages with a few spots of suitable glue.

3.2. Useful table packages

Modern LaTeX comes with several packages for tables that provide additional functionality. Below we mention a few. See the documentation of the individual packages for more details. The

Table 2: The next-to-leading order (NLO) results *without* the pion field.

Λ (MeV)	140	150	175	200	225	250	Exp.	v_{18} [?]
r_d (fm)	1.973	1.972	1.974	1.978	1.983	1.987	1.966(7)	1.967
Q_d (fm^2)	0.259	0.268	0.287	0.302	0.312	0.319	0.286	0.270
P_D (%)	2.32	2.83	4.34	6.14	8.09	9.90	–	5.76
μ_d	0.867	0.864	0.855	0.845	0.834	0.823	0.8574	0.847
$\mathcal{M}_{\rm M1}$ (fm)	3.995	3.989	3.973	3.955	3.936	3.918	–	3.979
$\mathcal{M}_{\rm GT}$ (fm)	4.887	4.881	4.864	4.846	4.827	4.810	–	4.859
$\delta_{\rm 1B}^{\rm VP}$ (%)	−0.45	−0.45	−0.45	−0.45	−0.45	−0.44	–	−0.45
$\delta_{\rm 1B}^{\rm C2:C}$ (%)	0.03	0.03	0.03	0.03	0.03	0.03	–	0.03
$\delta_{\rm 1B}^{\rm C2:N}$ (%)	−0.19	−0.19	−0.18	−0.15	−0.12	−0.10	–	−0.21

The experimental values are given in ref. [4].

Table 1
The next-to-leading order (NLO) results *without* the pion field.

Λ (MeV)	140	150	175	200
r_d (fm)	1.973	1.972	1.974	1.978
Q_d (fm^2)	0.259	0.268	0.287	0.302
P_D (%)	2.32	2.83	4.34	6.14
μ_d	0.867	0.864	0.855	0.845
$\mathcal{M}_{\rm M1}$ (fm)	3.995	3.989	3.973	3.955
$\mathcal{M}_{\rm GT}$ (fm)	4.887	4.881	4.864	4.846
$\delta_{\rm 1B}^{\rm VP}$ (%)	−0.45	−0.45	−0.45	−0.45
$\delta_{\rm 1B}^{\rm C2:C}$ (%)	0.03	0.03	0.03	0.03
$\delta_{\rm 1B}^{\rm C2:N}$ (%)	−0.19	−0.19	−0.18	−0.15

The experimental values are given in ref. [4].

packages can be found in LaTeX's `tools` directory.

`array` Various extensions to LaTeX's `array` and `tabular` environments.

`longtable` Automatically break tables over several pages. Put the table in the `longtable` environment instead of the `table` environment.

`dcolumn` Define your own type of column. Among others, this is one way to obtain alignment on the decimal point.

`tabularx` Smart column width calculation within a specified table width.

`rotating` Print a page with a wide table or figure in landscape orientation using the `sidewaystable` or `sidewaysfigure` environments, and many other rotating tricks. Use the package with the `figuresright` option to make all tables and figures rotate in clockwise. Use the starred form of the `sideways` environments to obtain full-width tables or figures in a two-column article.

3.3. Line drawings

Line drawings may consist of laser-printed graphics or professionally drawn figures attached to the manuscript page. All figures should be clearly displayed by leaving at least one line of spacing above and below them. When placing a figure at the top of a page, the top of the figure should align with the bottom of the first text line of the other column.

Do not use too light or too dark shading in your figures; too dark a shading may become too dense while a very light shading made of tiny points may fade away during reproduction.

All notations and lettering should be no less than 2 mm high. The use of heavy black, bold lettering should be avoided as this will look unpleasantly dark when printed.

3.4. PostScript figures

Instead of providing separate drawings or prints of the figures you may also use PostScript files which are included into your LaTeX file and printed together with the text. Use one of the packages from LaTeX's `graphics` directory: `graphics`, `graphicx` or `epsfig`, with the `\usepackage` command, and then use the appropriate commands (`\includegraphics` or `\epsfig`) to include your PostScript file.

The simplest command is:
`\includegraphics{file}`, which inserts the PostScript file `file` at its own size. The starred version of this command:
`\includegraphics*{file}`, does the same, but clips the figure to its bounding box.

With the `graphicx` package one may specify a series of options as a key–value list, e.g.:

```
\includegraphics[width=15pc]{file}
\includegraphics[height=5pc]{file}
\includegraphics[scale=0.6]{file}
\includegraphics[angle=90,width=20pc]{file}
```

See the file `grfguide`, section "Including Graphics Files", of the `graphics` distribution for all options and a detailed description.

The `epsfig` package mimicks the commands familiar from the package with the same name in LaTeX2.09. A PostScript file `file` is included with the command `\psfig{file=file}`.

Grey-scale and colour photographs cannot be included in this way, since reproduction from the printed CRC article would give insufficient typographical quality. See the following subsections.

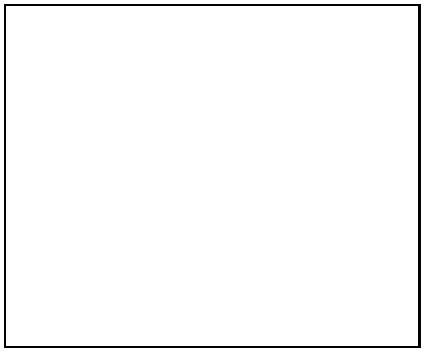

Figure 1. Good sharp prints should be used and not (distorted) photocopies.

3.5. Black and white photographs

Photographs must always be sharp originals (*not screened versions*) and rich in contrast. They will undergo the same reduction as the text and should be pasted on your page in the same way as line drawings.

3.6. Colour photographs

Sharp originals (*not transparencies or slides*) should be submitted close to the size expected in publication. Charges for the processing and printing of colour will be passed on to the author(s) of the paper. As costs involved are per page, care should be taken in the selection of size and shape so that two or more illustrations may be fitted together on one page. Please contact the Author Support Department at Elsevier (E-mail: `authorsupport@elsevier.nl`) for a price quotation and layout instructions before producing your paper in its final form.

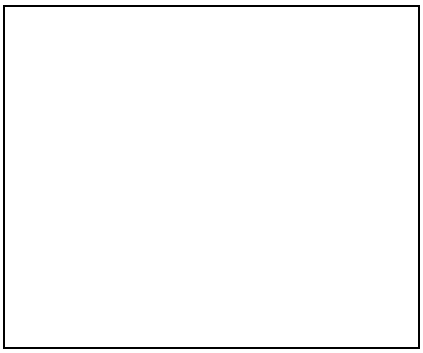

Figure 2. Remember to keep details clear and large enough.

4. EQUATIONS

Equations should be flush-left with the text margin; LaTeX ensures that the equation is preceded and followed by one line of white space. LaTeX provides the document class option `fleqn` to get the flush-left effect.

$$H_{\alpha\beta}(\omega) = E_{\alpha}^{(0)}(\omega)\delta_{\alpha\beta} + \langle\alpha|W_{\pi}|\beta\rangle \tag{1}$$

You need not put in equation numbers, since this is taken care of automatically. The equation numbers are always consecutive and are printed in parentheses flush with the right-hand margin of the text and level with the last line of the equation. For multi-line equations, use the `eqnarray` environment.

For complex mathematics, use the $\mathcal{AMS}$math package. This package sets the math indentation to a positive value. To keep the equations flush left, either load the `espcrc` package *after* the $\mathcal{AMS}$math package or set the command

`\mathindent=0pt` in the preamble of your article.

REFERENCES

1. S. Scholes, Discuss. Faraday Soc. No. 50 (1970) 222.
2. O.V. Mazurin and E.A. Porai-Koshits (eds.), Phase Separation in Glass, North-Holland, Amsterdam, 1984.
3. Y. Dimitriev and E. Kashchieva, J. Mater. Sci. 10 (1975) 1419.
4. D.L. Eaton, Porous Glass Support Material, US Patent No. 3 904 422 (1975).

References should be collected at the end of your paper. Do not begin them on a new page unless this is absolutely necessary. They should be prepared according to the sequential numeric system making sure that all material mentioned is generally available to the reader. Use `\cite` to refer to the entries in the bibliography so that your accumulated list corresponds to the citations made in the text body.

Above we have listed some references according to the sequential numeric system [1,2,3,4].

Study of CMS sensitivity to neutrinoless τ decay at LHC

R.Santinelli [a]

[a]Physics Department, University of Perugia and INFN Perugia,
1 via Pascoli, 06100 Perugia, Italy

The Large Hadron Collider (LHC), scheduled to start operation in 2006, is foreseen to provide in the first year of running a total of $\sim 10^{12}$ τ leptons.
CMS (Compact Muon Solenoid) is a general-purpose experiment designed to study proton-proton and heavy-ion collisions at LHC. Even if the Susy particles and Higgs searches togheter with the B-physics present its main goal, the large amount of τ-lepton, could allow a systematic study of tau-physics. We have performed a full simulation of CMS using GEANT 3 package and the object-oriented reconstruction program ORCA to study the sensitivity to neutrinoless tau decay $\tau \to \mu^+\mu^-\mu^-$ and $\tau \to \mu\gamma$. We present the analysis developed for these channels and the results obtained.

1. THEORETICAL INRODUCTION

In the Standard Model the neutrinoless decay of tau lepton are not foreseen because they would violate the *Charged Lepton Flavour* and/or the *Baryonic Number*. Until now there is no experimental evidence for such processes. The Noether theorem states that for every conservation law there must an associated symmetry and conversely. In the Standard Model we do not have a symmetry associate to the Charged Lepton Flavor Conservation law. It is simply a built in characteristics of the theory. Beyond the SM a large number of existing theories, can explain and accomodate them. An uncomplete list will include the Standard Model with right handed neutrinos, the Fourth generation neutrino theory, See-Saw type II models, GUT-theory, Susy with R-parity broken, Super Strings theories, Leptoquarks, Technicolor.
Every model in the above list provides or too an optimistic or too a pessimistic expectation of the neutrinoless decay Branching Ratios. Nevertheless, under the experimental point of view, the mSUGRA scenario with right handed neutrinos offers the closest forecast to the future experimental sensitivity. In this theory the vertices causing the violation of charged lepton flavour are due to non diagonal terms in the sleptons matrix mass which cannot be diagonalized simultaneously with the mass matrix of neutrinos. Mixing vertices arise at 1-loop radiative corrections from Yukawa couplings between sleptons and neutrinos.[1] With an opportune choice of the input universal parameters and with a texture describing the mixing in neutrino sector in accordance with the Super Kamiokande experiment, it possible to find a value of the Branching Ratio for the $\tau \to \mu\gamma$ around 10^{-7} while a 200 times lower value is expected for the $\tau \to \mu^+\mu^-\mu^-$.

2. CMS

The main features of this detector are the strong (4 Tesla) magnetic field, ensuring high momentum resolution for charged track, the efficient muon system, providing a very good reconstruction of muon and the very small global size.
The detector consists of a silicon tracker with an embedded pixel detector, a crystal $PbWO_4$ electromagnetic calorimeter (ECAL) and a copper-scintillator hadron calorimeter(HCAL). A sophisticated four station muon system made of tracking chambers, the drift tube (DT) and the cathode strip chamber (CSC) and of dedicated trigger chamber (the resistive plate chamber or RPC), is located outside the solenoidal magnetic field. The overall dimensions of the CMS detector are: 21.6 m in length, 14,6 m in diameter with a to-

tal weight of 14,500 tons. Both the analysis I will present here will rely heavily on the performances of the muons subdetector for its high efficiency to detect isolated muons (95%) and its low probability to misindentify pions or kaons as muons.

Another very important component of CMS detector is its tracking system. The performances of the CMS tracker play a fundamental role in the improvement of the Branching Ratio sensitivity to tau in three muons decay channel.

The main requirements are:

- high radiation resistance because the tracker will be the part of CMS closest to the primary interaction point and it will be therefore operating in a very high radiation enviroment
- a low material budget, to minimize the photon conversion and bremsstrahlung.
- high momentum resolution
- high secondary vertex reconstruction efficency

The expected resolution on the transverse momentum of muons will be $\frac{\sigma_{Pt}}{Pt}$ =1.5% for 10 GeV muons and the resolution on the secondary vertex reconstruction about 200 μm. The particle detection efficiency is expected to be 95% for isolated charged tracks and 90% for tracks inside a jet.

As for what regards the calorimeters, they become of the ut most importance in the $\tau \rightarrow \mu\gamma$ analysis, where we require a good photon reconstruction.
The transverse energy resolution for electron/photon could be parameterized as:

$$\frac{\sigma_E^{ECAL}}{E} = \frac{a}{\sqrt{E}} \otimes b \otimes \frac{c}{E} \quad (1)$$

The "stochastic term" a arises from photoelectron statistics and shower fluctuaction. The "constant term" b has contributions from non-uniformities and from shower leakage. The "noise term" c is due to electronics noise and pile-up. The design goal for the CMS ECAL barrel and endcaps are a = 2.7% and a = 5.7% respectively and $b <$ 0.55% for both section of the detector. Expressing the noise as trasverse energy, the goals for the c term are at low luminosity c=155MeV for the barrel part and 205MeV for the end-caps. The phi-angle resolution is expected to be 1.3 mrad.

3. $\tau \rightarrow \mu^+\mu^-\mu^-$

In Table 1 we summarize the main sources of tau leptons at LHC as we have found using PYTHIA 6.152 generator and the branching ratio listed in the PDG tables.

The total cross section will be of around 120 μb for a total amount of tau produced after one year of low luminosity of LHC (integrated luminosity of 10 fb^{-1}) of 10^{12} tau lepton. Because we will only be capable to trigger on the higt p_t particles, we have concentrated on the following signal sources:

- W source, $\sigma(pp \rightarrow W \rightarrow \tau\nu_\tau)$=19 nb [2]
- Z source, $\sigma(pp \rightarrow Z \rightarrow \tau\tau)$=3nb
- B source, $\sigma(pp \rightarrow B \rightarrow \tau D\nu$=24$\mu$b

The W source, as we shall see, represents the best source for the signal.

3.1. The background

The presence of three well reconstructed, collimated and isolated muons offers a very clear signature for the signal. According to the results of [3] the main sources of μ that could contribute to the background will be:

- heavy quarks mesons (D & B)
- pile-up effects from primary interaction
- Gauge bosons and Drell Yan (Z,W)
- τ production
- cosmic rays
- Susy Particles
- Higgs decay

Table 1
Main sources of τ-leptons at LHC

Meson (M)	D_S	D^+	B^0	B_S	B^+
BR($M \to \tau + X$)	7.0%	0.2%	2.7%	1.5%	2.7%
$\sigma(M \to \tau + X)/\sigma(pp \to \tau + X)$	77%	3%	9%	2%	9%

- non prompt muons (punchthrough pions non interacting in the calorimeters)

Pile-up effects from primary interaction and tau source of muons are not considered for their low probability to have a final three muons topology. The cosmic rays will be removed by timing. W and Z source will give negligible contribution due to their distinctive high mass. Susy particles and Higgs sources present a too low total production cross section to be really dangerous at the present sensitivity attainable.
We focused then on heavy quarks mesons and on unphysical background. Events were simulated using the PYTHIA [6] kinematics generation followed by the GEANT3 ([8]) based simulation program CMSIM ([7]) and the reconstruction program ORCA ([9]).

3.2. Heavy quarks mesons events

We focus our investigations over events with only 3 muons in the final state. This kind of events can occur in two different ways as depicted in fig. 1

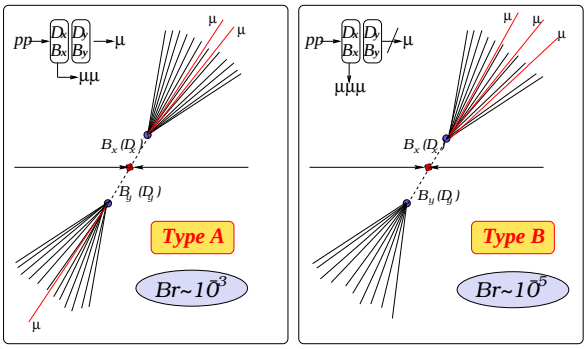

Figure 1. Three muons from $b\overline{b}$ and $c\overline{c}$ events

A preliminary study, conducted at kinematic generation level, has shown that an upper cut on the angle between two muons removes completly events of type A, leaving almost all the events of type B. These can be generated by forcing decay cascades where some resonances rare decay should be included like $\phi \to \mu\mu$ For the background we forced the following decays

- $pp \to D_X D_S \to D_X \mu\nu_\mu \phi \to D_X \mu\nu_\mu \mu\mu$
- $pp \to B_X B_S \to B_X \mu\nu_\mu D_S \to B_X \mu\nu_\mu \mu\mu K$

It is worthwhile to note that the choice of the ϕ as the resonance decaying into 2 μ is not unique, but one of the most important. We could use other resonances like ω, η, η' but their contribution will be too small. Moreover, to increase the final statistics, we required, at the generation level, three muons with a transverse momentum greater than 3 GeV. We will refer to these events as *preselected*. Finally, we obtained from a fast simulation, the very important information that the $b\overline{b}$ events are negligibile if compared with $c\overline{c}$. This is true because the reconstructed final three muons mass for $b\overline{b}$ events is shifted toward 4-5GeV values while the one from $c\overline{c}$ is peaked around 1.5 GeV.
We will consider then the events $pp \to D_X D_S \to D_X \mu\nu_\mu \phi \to D_X \mu\nu_\mu \mu\mu$ as the main source of background (*main background*)

3.3. Signal and analysis

Different τ-sources give rise to different signal signatures. We have therefore adopted three different set of cuts appropriates for the different sources of signal.

3.3.1. τ from W

These events are mainly characterized by an high value of missing energy. Indeed the tau coming from W decay shares half of the initial boson's energy with the corresponding neutrino and this will be detected as an high missing energy, (see fig. 2)

Here we have for the signal from W the typical Jacobian peak around 35 GeV while the distribution is shifted toward low values for the main background and for the signal from Z. The complete analysis implemented for these events require:

- trigger
  1. at least 3 muons passing the CMS trigger level 1 (L1)
  2. 2 or more CMS level 3 muons (the final CMS trigger level for muons) (L3)
- identification
  1. only 3 well reconstructed and close muons candidates from tracker with a Pt>4GeV in the barrel region and Pt>2.5GeV in the endcaps
  2. total charge equal ± 1
- topology
  1. Common secondary vertex (not necessary to implement!)
  2. no charged tracks inside a cone of $\Delta R = \sqrt{\Delta\phi^2 + \Delta\eta} = 0.4$ around the μ tracks. (ϕ is the azimuthal angle and η is the pseudorapidity).
- missing transverse energy >20GeV
- veto on phi-mass region (1020±25)MeV for any couple of muons
- reconstructed three muons mass =1778±20MeV

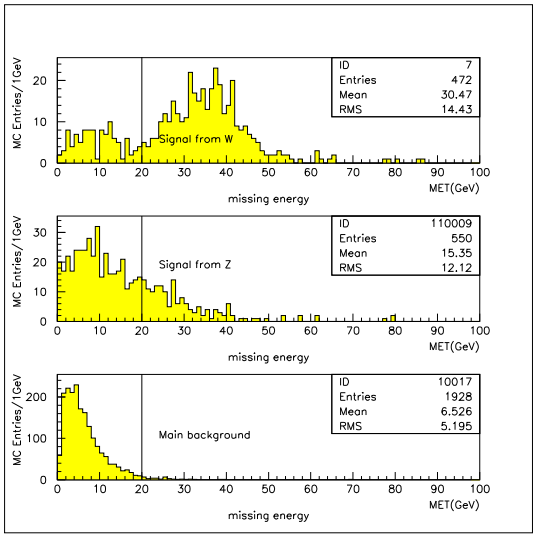

Figure 2. Transverse missing energy

The isolation cut is justified by the high multiplicity of background events and the low number of tracks for this kind of signal. In figure 3 we compare the number of tracks around the three muons for the signal from W, for the background and for the signal from B. Once again we would remove a large number of events from this source by excluding the events with other charged tracks around the three muons.

In figures 4 and 5 we illustrate the secondary vertex cut and the veto on phi mass. The probability to have three muons from a common secondary vertex is shown in figure 4. From this figure we also see how signal and cc events present the same distribution while, as expected, the bb events have a peak at zero. In this case the muons pair originating from Ds decay presents a vertex position distinct from the origin position of the third muon coming directly from Bs decay. The dimuon-mass plot for signal and main background are self-explaining and do not need any other comment. Finally we remove all the background events by applying the three muons mass cut where the resolution found for the sig-

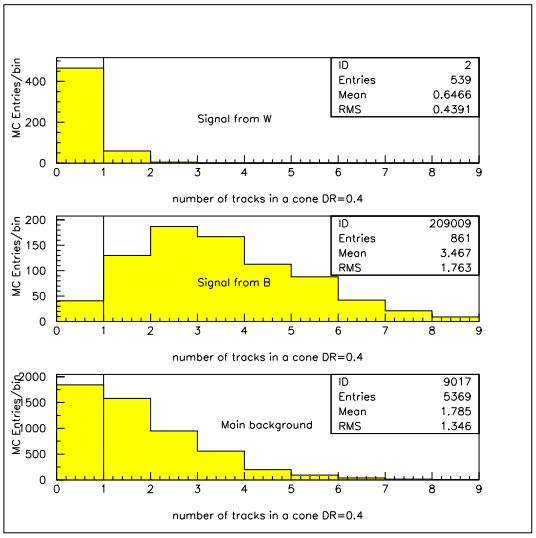

Figure 3. Number of track inside a cone of opening =0.4 around the three muons

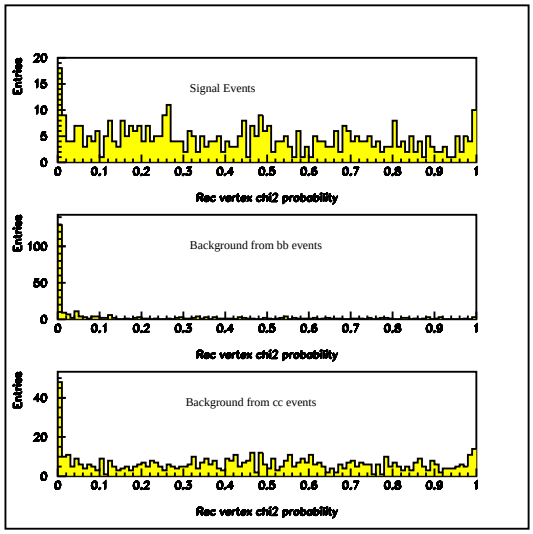

Figure 4. Reduced chi squared probability of three muons to belong to same vertex

nal is 15MeV. At the end of the analysis, with the hypothesis that the BR of tau in three muons is the actual experimental limit set by CLEO II (1.9×10^{-06}), we expect after one year 44±2 signal events against 1±1 of the background. In fig 6 we illustrate the plot of the signal plus background and background as expected with an integrated luminosity of $10fb^{-1}$ (available after one year of LHC running at $\mathcal{L} = 10^{33}cm^{-2}s^{-1}$) and assuming the Branching Ratio to be equal the present CLEOII experimental limit. This will correspond to an upper limit on the BR (at 90% CL) of 8.4×10^{-8}.

3.3.2. τ from Z and from B

In this case we can exploit the second tau which is selected by applying a second isolation criterium based on the fact the tau usually decay in one or three well collimated charged tracks. Moreover this tau and the tau signal will give the reconstructed Z-mass. The analysis used for this source is quite similar to that of the W source with the main difference that we do not apply the missing energy cut but we require the following additional cuts:

- second tau isolation (1 to 3 tracks inside a narrow cone of 0.03 aperture and no other tracks inside a broader and complementary cone of opening 0.4 with Pt>1.5
- Pt_τ >23GeV
- reconstructed mass of the tau-jet+ missing energy+three muons greater than 70GeV

In figure 7 we have a summary of the Z-dedicated set of cuts. In the upper part we have the distribution for the signal while in the bottom that for main background.

Because of the lower Z cross section production, the final number of events from Z surviving our analysis will be 4±1 and 0.8±1 the background events for $10fb^{-1}$. The corresponding sensitivity if no signal is detected will be 7.6×10^{-7}.

The final sorce of signal considered was the B. At low luminosity regime of collider this could be

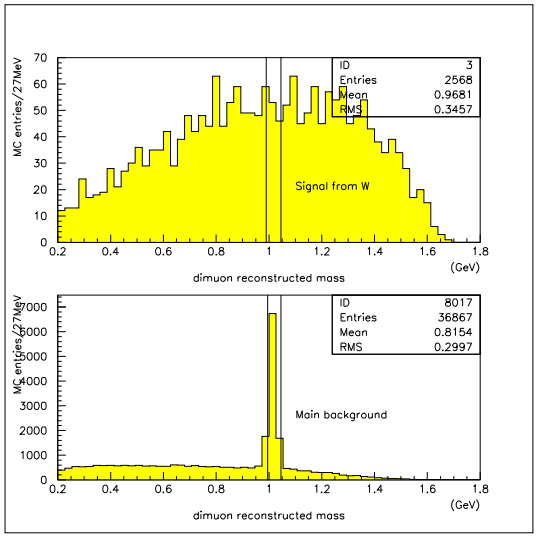

Figure 5. Combinatorial dimuon mass

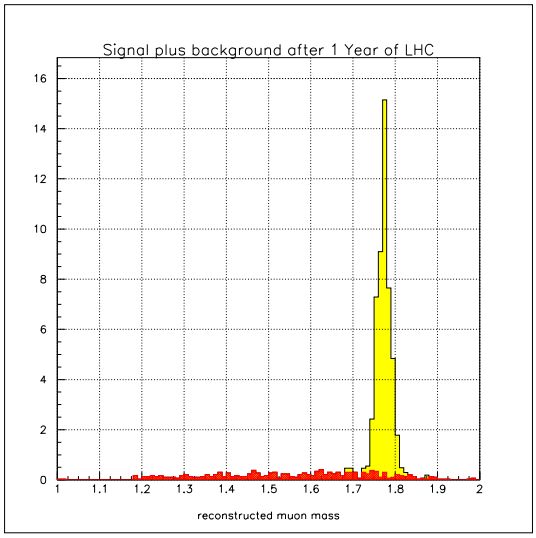

Figure 6. Signal plus background after one year of luminosity of LHC assuming a BR equal to the CLEOII limit

a very important source of signal. These events present a signature completly different from the previous ones. First, their multiplicity is too high to apply isolation cut and the missing energy selection can not be applied. Second the energy of the tau is not so high to be a good cut candidate. In this case after the trigger and the identification criteria, we therefore require two consecutive b-tag for the two b-jet candidate. The b-tag alghorithm considered was the simplest possible one by requiring some track for every events inside a jet with a significance of the transverse impact parameter greater than a given value to tune. In figure 8 we show this variable for the three muons jet for signal events (top) and main background (bottom). We cut out events presenting less than 3 tracks with significance of impact parameter greater than 2. With this analysis we can to reach a sensitivity of BR at 90% equal 3.8×10^{-7}.

3.4. Instrumental background

Till now we estimated the sensitivity by considering only physical channels whose experimental signature is closest to that of the signal. However, tied to very low sensitivity we would reach, it is dangerous to exclude a priori other source of background arising in an experimental environment. Although,(see [4]), the estimation of the probability to mistag at CMS trigger level 1 a light meson (pion or kaon) as muon is very low ($\sim \frac{1}{100}$) and decreases with the threshold on the roughly reconstructed level 1 transverse momentum of the particle, we have done a systematic analysis to evaluate their contribution. First we generated 500 events, as kinematically close as possible to the signal, and considered the decay $\tau \rightarrow \pi\pi\pi\nu_\tau$ (with the tau from W) replacing two pions with two real muons. In this way we are able to estimate the probability to mistag the third π as μ by simply counting how many close muons have been reconstructed by our simulation program at level 1 or 2 or 3. In figure 9 we show these numbers.

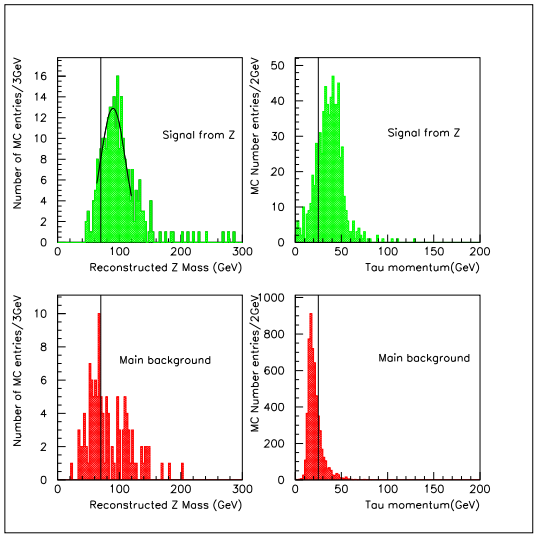

Figure 7. Main kinematical variables used for the Z-dedicated analysis

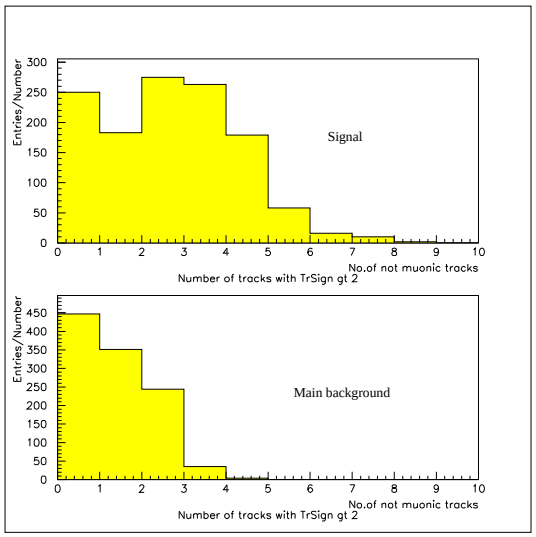

Figure 8. Number of tracks with a significance of IP greater than 2

We found at level-1 that 5 events (among 500) present 3 μ. We can then estimated a 1% misedintification probability.
After this cross-check, we have considered as background the following channel, $\tau \rightarrow \pi\pi\pi\nu_\tau$, with all the three pions misidentified as muons. The expected number of events passing after one year the analysis (W dedicated) is given by the formula:

$$N_{1year} = \mathcal{L} \times BR(pp \rightarrow W \rightarrow \tau\nu) \times BR(\tau \rightarrow \pi\pi\pi\nu) \times P(\pi \rightarrow \mu)^3 \times \epsilon_{analysis} \quad (2)$$

With $\epsilon_{analysis} \simeq 10^{-3}$ and BR$\sim$ 9%, we found for these events an expected rate negligible compared with the physical background.

4. $\tau \rightarrow \gamma\mu^-$

Encouraged by the previous results we have undertaken a preliminary study of the possibility to detect the $\tau \rightarrow \mu\gamma$ decay channel, which is expected to be much higher even if much harder to be detected experimentally. We have focused on the τ source which allows to exploit the large missing energy expected. So the background has to be seeked inside muons sources with high missing energy. The same background should have a very hard and well isolated muon. From these preliminary considerations we focused our attention to the following events:

- $pp \rightarrow W \rightarrow \mu\nu_\mu$ (SAMPLE A $\sigma = 19nb$)
- $pp \rightarrow W\gamma \rightarrow \mu\gamma\nu_\mu$ (SAMPLE B $\sigma = 0.18nb$)
- $pp \rightarrow W \rightarrow \tau\nu_\tau \rightarrow \mu\nu_\mu\nu_\tau\nu_\tau$ (SAMPLE C $\sigma = 2.1nb$)

These events present similar kinematical features although some important differences arise. The sample A present the highest cross section. The photon presence is not assured and eventually it could come from some π^0. The sample B, with a photon radiated from primary interaction, present a cross section 100 times smaller. The muon is very hard and the photon is not always close to muon. The sample C is expected to have the most signal like distributions and then the rejection power to be the poorest among the

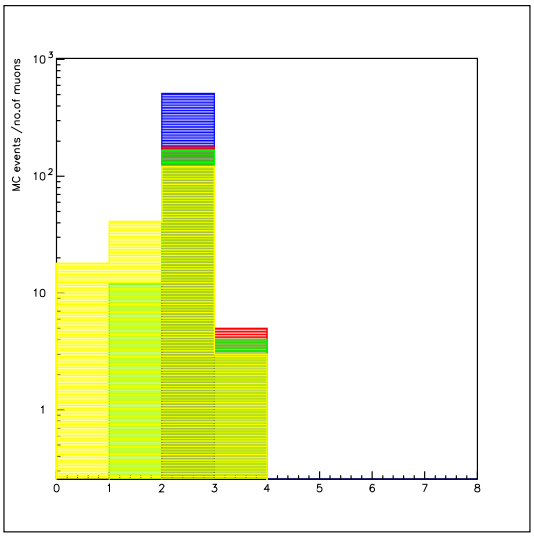

Figure 9. Number of real, L1, L2 and L3 reconstructed muons

channels considered. The analysis steps are the following

- Level 1 trigger
  1. 1 photon with L1 $E_T > 25$ GeV or
  2. 1 muon with L1 $p_T > 20$GeV or
  3. 1 muon with L1 $p_T > 5$GeV and 1 photon with L1 $E_T > 15$ GeV
- high level trigger:1 well reconstructed photon (level 2) and one muon L3 or just one high transverse momentum track close to the photon
- reconstructed transverse energy of photon greater than 18 GeV
- missing transverse energy greater than 20 GeV
- candidate muon momentum less than 20 GeV
- angular distance between muon and photon greater than 008 and less than 0.15
- significance of impact parameter of muon greater than 2
- reconstructed mu-gamma mass equal the tau mass $\pm$ 60MeV

In figure from 10 to 12 we illustrate the distributions of the quantities used in the analysis. The sample C of background is shown in dashed line in figures 10 and 11. In solid line we plotted the same variables for sample A events and in dotted line for sample B. We note that the sample C shows distributions for the μ momentum and transverse impact parameter closest to these for the signal. In figure 12 and 13 we plotted the transverse energy of photon for the signal (filled area) and for the background (solid line) and angular distance between muon and photon. We avoided to show for these quantities the distribution for sample B and C whose shape is similar to the sample A.

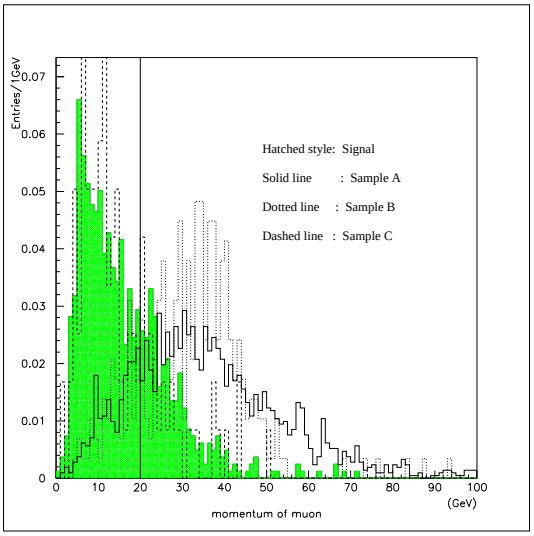

Figure 10. Muon momentum distribution

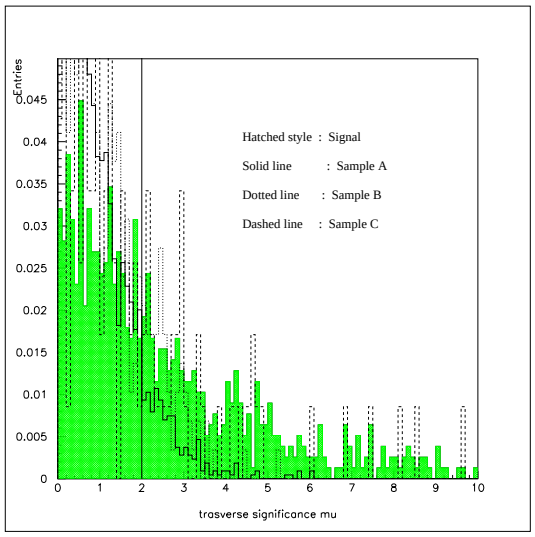

Figure 11. Muon transverse impact parameter significance distribution

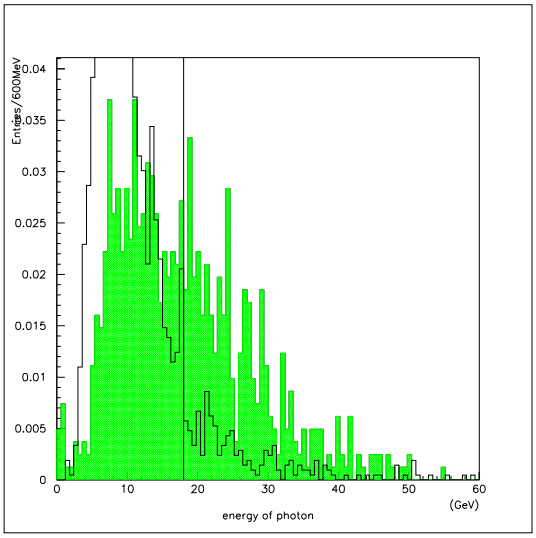

Figure 12. Photon transverse impact energy distribution (filled area for the signal)

In figure 14 we present the photon-muon reconstructed mass for the signal events. We also plot the mass region around the tau mass which shows a resolution of around 40 MeV. (this is worse than one found in CLEOII and Atlas collaboration [5]) At the end of the analysis we still remain with around a 6% of MonteCarlo initial signal events produced and we remove all the initial 40000 events of sample A and 3500 events of sample B and C. The normalized number of background events expected after one year is 13 from sample A, less than 1 from B and 18 events from sample C which is confirmed to be the most dangerous background. To find these numbers we adopted the hypothesis the mass distribution for the background is uniform in the range between 0 to 3 GeV. This is a rather pessimistic hypothesis, because the mass for the background (upper box in fig. 15) is peaked below 1 GeV/c^2 and in the interesting region (τ-mass $\pm$ 60MeV/c^2) the number of events is smaller than the one foreseen with a flat distribution assumed. With these assumptions we evaluated the BR to be less than 10^{-6} for the $\tau \to \mu\gamma$ after one year of low luminosity of LHC taking data.(10 fb^{-1})

5. Conclusion

We have presented the MonteCarlo based analysis of neutrinoless decays channel $\tau \to \mu^+\mu^-\mu^-$ and $\tau \to \mu\gamma$ using the CMS object-oriented reconstruction program ORCA. We isolated and analysed three important sources of signal. We found that the most dangerous background for the first channel is represented by $c\overline{c}$ events with three muons coming from a common meson. After one year of low luminosity of LHC we could improve by a factor 25 the actual experimental sensitivity to this channel by using only the W source. Other channels (Z and B) give a minor contribution in the present analysis. For the $\tau \to \mu\gamma$ channel the

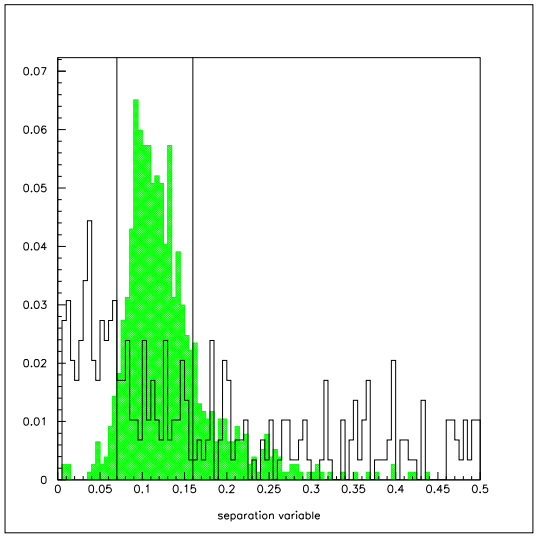

Figure 13. Photon-muon angular distance distribution (filled area for the signal)

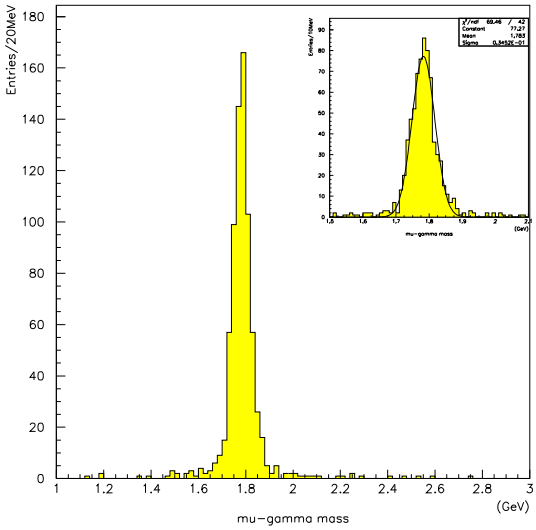

Figure 14. Signal muon-photon reconstructed mass

most dangerous background arises from leptonic decays of W boson and a first study confirm the results of ATLAS. The signal is background limitated and the CMS sensitivity for this analysis will be similar to that expected at the B factories. Nevertheless, more detailed studies of pile-up effects are required to extend the analysis to higher luminosity.

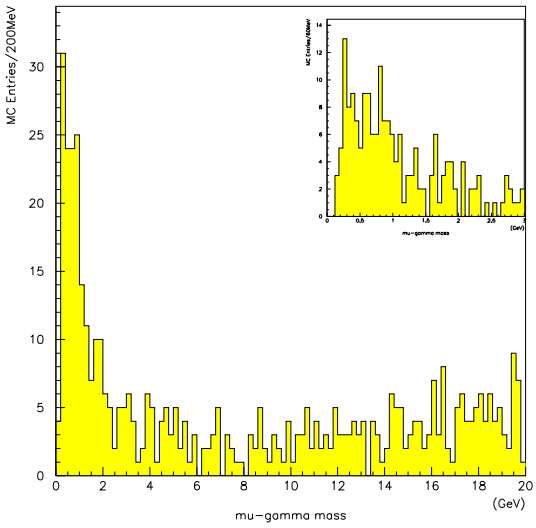

Figure 15. Background muon-photon reconstructed mass

REFERENCES

1. hep/ph 9911459 J.Ellis at al.
2. Nucl.Physics B345 331-368
3. CMS-NOTE 1997/096
4. CERN/LHCC 2000-38 CMS TDR 6.1
5. Atlas internal Note PHYS-97-114
6. T.Sjostrand, CERN-TH/7112/93
7. http://cmsdoc.cern.ch/cmsim/cmsim.html
8. Cern Program Library Writeup W5013
9. http://cmsdoc.cern.ch/orca